Advances in Physics Theories and Applications
ISSN 2224-719X (Paper) ISSN 2225-0638 (Online)
Vol.61, 2017

Study of the Scattering α-Projectiles at the Energy of $1 \leq E_\alpha \leq 10MeV$ on the Al^{27} Target Nucleus in the Framework of the Method of Variational Moment Approach (VMA)

Dr. Anees. B. Blal[1] Khadija .S.Alhassan[2]
1.Professor at Department of Physic, Faculty of Sciences, Albaath University, Homs-Syria
2.PhD candidate at the Department of Physics, Faculty of Sciences, Albaath University, Homs-Syria

Abstract
The Method of Variational Moment Approach (VMA) depends on the relation that connects the real and imaginary parts of the optical model potential, known as the causality-based dispersion relation, where the Causality Principle sets forth that a scattered wave cannot be transmitted before the arrival of the incident wave. In this Study, an attempt is made to extend the application of the VMA Method, which dealt with simple systems, such as the proton- nucleus system and the neutron-nucleus system, in order to study the dispersion of complex systems such as the nucleus-nucleus system at a low range of energy.
Wherefore, we found the following:

1. The values of the geometrical parameters for the optical model potential specified in accordance with this Method and for the $\alpha + Al^{27}$ interaction at the $1 \leq E_\alpha \leq 10MeV$ energy range are correlated with the energy of the projectile and the linear dependence;
2. After having calculated the real and imaginary momenta values $[r^2](E)$ in terms of energy, it is further found that the values of such momenta are typical to their referential counterparts;
3. After having calculated the values of the total reaction cross section and the differential reaction cross section and in dependence on such parameters using the SPI-GENOA program, it is found that they are approximating the experimental counterparts (those experimentally measured).
4. Through the study of the energy-dependent potential, it is also found that there is a deviation in its behavior in vicinity of the quantum energy barrier.

Introduction
The α-particle optical model potential plays a key role in the studies of nuclear structure and nuclear reactions. It is used to unify the bound and scattering α-particle states [1], to analyze the superheavy particles induced by the α-decay[2], which constitutes the fundamental basis for the applications of nuclear astrophysics, and for the estimation of the radiation damage effects ensuing from the concomitant fusion state and the accelerator–driven systems (ADS). Due to such importance of the α-particles optical model potential (OMP), trials were made in order to determine and figure out its shape by studying the mutual effects of the α-projectiles at a certain range of energy into the direction of the target nuclei, in search for a certain phenomenological method. In previous literature, the OMP of the α-projectiles at certain intermediate range of energies was determined well, and in order to ascertain the determined findings, the data, which was related to the scattering α-particles at low range of energies, were analyzed, and whereby it was found that the OMP parameters, obtained from α-particle elastic scattering at intermediate range of energies, [3.4] were invalid for the phenomenological description of the scattering α-particles for lower energies (<40 MeV).

Within the work [5] and upon analyzing the elastic scattering of the S^{32} heavy ions bombarded at the energy $E_{\alpha=[5-100-120-151]}$ MeV via the Ca^{40} nuclei, there has been, for the first time, reference to the Threshold Anomaly (TA) phenomenon. Within the work [6], an interpretation for the TA phenomenon is provided through the introduction of the dispersion relation that connects both real and imaginary parts of potential. The optical model (OM) is used in order to explicate the mechanism of mutual effects between the nucleons and the nucleus, to expound the properties of colliding particles at an intermediate range of energies, and to render an accurate determination of the potential parameters. Insomuch as the low-energy ranges are concerned and due to the unavailability of experimental data at that time about each of the $\sigma(\theta)$ energy-dependent reaction cross-section, polarization $P(\theta)$ and the $\sigma(E)$ energy-dependent total cross-section, the OM was hardly made use of in breaking down all such previous values. Notwithstanding, the OM was tantamount to be the basis that had been sprung from several works and literature, and from which were emanated results that constitute a key cornerstones for future works. In light of the foregoing, both Researchers [1.2.3] devised a

newly sophisticated model, which is systemized along the lines of the optical model, and which is called "the dispersive optical model" that incorporates two at-odds methods in principle: the Dispersive Optical Model method (DOMA) and the Variational Moment Approach (VMA) method. The former method involves the full description of potential by setting such potential on the basis of utilization of a full set of OP parameters, which is ideally selected while collating them with the elastic-scattering experimental data. The latter method was *ab initio* applied to study the mutual effects of $(P + Ca^{40})$, $(n + Ca^{40})$ and $(P, n + Pb^{208})$ at the low- and intermediate-ranges of energy. This method depends on the dispersion relation that connects both real and imaginary components of optical model potential leading to the reduction of the number of potential geometrical parameters required to be fathomed. This method is built on the analysis of the data that is related with the scattering nucleons of the $\sigma(\theta)$, $P(\theta)$ and $\sigma(E)$ in their entirety in order to determine the OP parameters.

This method was afterwards applied in order to study the optical and non-optical systems of $(P + A)$ and $(n + A)$ [7]that have got more than or less than one nucleon or two or three nucleons outside the closed shell, and less than one nucleon or two or three nucleons outside the closed shell respectively. In view of the successful results reached by this Method (i.e. the VMA method), we deemed it advantageous to extend it to incorporate the study of more complicated systems (that is to say, the nucleus-nucleus systems), an example of which is $({}_2^4He + A)$, and to build and figure out the shape of potentials through finding the geometrical parameters for such potentials at the low- and intermediate-ranges of energies since the preceding studies were mainly dependent on scrutinizing the values of intermediate energies.

Making use of the VMA method to study the scattering α-particles at low and intermediate ranges of energy would allow the interpretation of several reactions, at the top of which the interpretation of the deviation phenomenon near the Coulomb barrier. It would further interpret and render an explanation for the mass number and energy dependence of the imaginary potential and the estimation of the reaction total cross-section and differential at such ranges of energy.

Modus Operandi of Finding the OMP Parameters of the Nucleus-Nucleus System:

In the framework of the VMA method, the central part of the mean field *M (r, E)* resulting from the mutual effect of the nucleus-nucleus global system is topically local, and is expressed thereabout according to the following equation:

$$M(r,E) - V(r,E) + iW(r,E) + V_{ls}(r,E) + V_C(r) \quad (1)$$

The first term *M (r, E)*: it represents the real part of potential, which is composed of two components:

1. The V_0 *(r, E)* Component, which consists in an energy-related exponential function, and the shape thereof is smooth;
2. The Dispersive component, which is called the "Dispersive potential" (i.e. the "Dispersion Relation"). This relation connects both of the real and imaginary parts of potential, and is expressed in the following integral equation:

$$\Delta V(r,E) = V_0(r,E) + \frac{P}{\pi}\int_0^{\infty} \frac{W(r,E`)}{(E - E`)} dE` \quad (2)$$

Where: *P* is dependent on the principal value of the integrand;

The energy-dependent $\Delta V(r,E)$ relates mainly to energy. Consequently, the first term of Eq. (1) represents the summation of two terms; i.e.:

$$V(r,E) = V_0(r,E) + \Delta V(r,E)$$
$$= V_0(r,E) + \Delta V_{W_w}(r,E) + \Delta V_{W_d}(r,E) \quad (3)$$

It is to be known that the Dispersive potential has got two component; to wit, the surface and volume dispersive potentials, which are expressed as stated in Eq. (3).

As for the second term of Eq. (1): *W (r, E)* represents the imaginary part of the OP, which consists in the summation of two terms (i.e. the volume and surface imaginary potentials), and which is expressed in the following equation:

$$W(r,E) = W_W(\mathrm{r,E}) + W_d(r,E) \quad (4)$$

It is notable that both Eq. (2) and Eq. (3) are correlated with each other via the Dispersion Relation.

The third term of Eq. (1), $\Delta V_{ls}(r,E)$ represents the potential arising from the mutual effects between each spin of the incident particle and orbital momentum of the target nucleus.

The forth term of Eq. (1), $V_c(r)$, represents the optical potential (OP).

Due to the disparity of the OP parameters, reproduced by the energy analysis of the experimental data pertaining to the reaction cross-sections, and the rendition of a value commensurate with the reaction cross-sections, it behooved to search for some coefficients that help reduce the number of parameters on one hand and eliminate ambiguity on the other hand through determining them. These coefficients are known as the second-order moments of optical potential (the volume integrals per nucleon). These moments render an in-depth understanding of the behavior of the energy-dependent optical potential [8]:

1- The second-order Moment of the Real-Part Potential $J_V(E)$

2- The second-order Moment of the imaginary-Part Potential $J_w(E)$

And the second-order dispersive moment, where the second-order moment of the imaginary-part Potential is determined in the framework of the VMA method by the following equation:

$$J_w(E) = J_{w_w}(E) + J_{w_d}(E) \quad (5)$$

$$= \frac{4\pi}{A_P A_t}\int_0^{\infty} W_d(r,E) + W_W(r,E) r^2 dr \quad (6)$$

J_{w_w} : It represents the second-order moment of the volume imaginary potential;

J_{w_d} : It represents the second-order moment of the volume surface potential;

Returning to the second-order moment of the total imaginary potential $J_W(E)$ the volume imaginary potential J_{w_w} by the Brown-Rho Scaling Relation [9], it is expressed as follows:

$$J_W(E) = \beta_2 \frac{(E-E_0)^2}{(E-E_0)^{2+\rho_2^2}} \quad (7)$$

$$J_{W_W}(E) = \beta_2 \frac{(E-E_0)^2}{(E-E_0)^{2+\rho_W^2}} \quad (8)$$

Where $(\rho_W, \rho_2, \beta_2)$ consist in parameters that are set by the way of identifying $J_W(E)$ for the sake of eliciting different values of energy with the same value thereof $J_W(E)$, which is calculated by using the classic Optical Model (TOM). We will tackle the explanation of E_0=0 later on.

As for the second-order surface imaginary moment of the surface imaginary potential, $J_{W_d}(E)$, it is determined by the difference of $J_{W_W}(E)$ and $J_W(E)$ as follows:

$$J_{W_d}(E) = \beta_2 \left[\frac{(E-E_0)^2}{(E-E_0)^2+\rho_2^2} - \frac{(E-E_0)^2}{(E-E_0)^2+\rho_W^2}\right] \quad (9)$$

Having calculated the second-order moments of the volume, surface and total imaginary potentials in line with the preceding equation, we can afterwards find out the imaginary potential with both of its volume and surface imaginary parts as follows:

$$J_{W_W}(E) = \frac{4\pi R_W^3}{3A_P A_t}\left[1 + \frac{1}{3}\left(\frac{\pi a_w}{R_W}\right)^2\right] W_w(E) = g_{w_w} W_{w_w}(E) \quad (10)$$

Where it is known that:

$$g_{w_w} = \frac{4\pi R_W^3}{3A_P A_t}\left[1 + \frac{1}{3}\left(\frac{\pi a_w}{R_W}\right)^2\right] \quad (11)$$

A_t & A_p represent respectively the mass numbers of the target nucleus and the projectile.

$R_w = r_w A^{\frac{1}{3}}$

$$J_{W_d}(E) = \frac{4\pi}{3A_P A_t}(12 a_d R_d^2)\left[1 + \frac{1}{3}\left(\frac{\pi a_d}{R_d}\right)^2\right] W_d(E) = g_d W_d(E) \quad (12)$$

While it is known that:

$$g_{w_d} = \frac{4\pi}{3A_P A_t}(12a_d R_d^2)\left[1+\frac{1}{3}\left(\frac{\pi a_d}{R_d}\right)^2\right] \quad (13)$$

It is apparently notable that the finding of energy dependencies of both $W_d(E)$ and $W_W(E)$ relies on determination of the values of the reproduced parameters $(a_w\ a_d\ r_w, r_d\ )$, which are included in the fitting of g_{w_d} and g_{w_w}, as mean values.

As for the real part of the central potential, it is composed of the summation of two terms as stated in Eq. (3):

$V(r,E) = V_0(r,E) + \Delta V(r,E)$

$\Delta V(r,E)$: It determines the Dispersion Relation (DR), which connects both of the real and imaginary parts of potential as shown in the following equation:

$$\Delta V(r,E) = \frac{2}{\pi}(E-E_S)\int_{E_0}^{\infty}\frac{W(r,E`)}{(E-E_S)^2-(E`-E_S)^2}dE` \quad (14)$$

The dispersive potential is composed of the summation of two term; i.e. the surface dispersive potential ΔV_d and the volume dispersive potential ΔV_w.

$$\Delta V(r,E) = \Delta V_W(E)f(r_w) += \Delta V_d(E)g(r_d) \quad (15)$$

They are determined in accordance with the following Dispersion Relation:

$$\Delta V_W(E) = \frac{2}{\pi}(E-E_S)\int_{E_0}^{\infty}\frac{J_{W_W}(E`)dE`}{g_{W_W}(E`)[(E-E_S)^2-(E`-E_S)^2]} \quad (16)$$

$$\Delta V_d(E) = \frac{2}{\pi}(E-E_S)\int_{E_0}^{\infty}\frac{J_{W_d}(E`)dE`}{g_{W_d}(E`)[(E-E_S)^2-(E`-E_S)^2]} \quad (17)$$

E_s represents a reference energy, for which the second-order moment of potential $V_0(E_S)$ is to be set on the assumption that $g_W(E)$ and $g_d(E)$ are not correlated with the value of E. For the convenience of calculations, we can go beyond the integral reference and operate the preceding integral equation, taking into cognizance that each of $f(r_w)$ and $g(r_d)$ has the form of the Woods-Saxon (WS) dependence shape, and are determined by the following equations:

$$f(r_w) = [1+\exp(x_w)]^{-1} \quad ; x_w = \frac{r-R_w}{a_w}; \quad R_{W=}\, r_w A^{1/3} \quad (18)$$

$$f(r_d) = -a_d\ \frac{df(x_d)}{dr}\ ; x_d = \frac{r-R_d}{a_d}; \ R_{d=}\, r_d A^{1/3} \quad (19)$$

In the framework of the VMA method, the parameters $a_w\ a_d\ r_w, r_d$ are required to be taken as mean and homogeneous values, that is to say:

$a_d = r_w$: $r_d = r_w$

After determining the dispersive component of the real part (namely, the second term in Eq. (3)), we move to the determination of the first term (namely, $V_0(r, E)$), which is identified according to the following equation:

$$V_0(r,E) = U_0(E)\,f(r) \quad (20)$$

$f(r)$: It is determined by use of an equation being similar to Eq. (18).

As we mentioned hereinabove, $V_0(r, E)$ relies on energy and the dependence thereof due to substituting the nonlocal potential with a local equivalent as the nuclear power affects a newly localized location.

The potential depth $U_0(E)$ is given the following formula [Ca^{40}]:

$$U_0(E) = U_0(E_S)\exp\alpha\ (E-E_S) \quad (21)$$

Nevertheless, the second-order moment of the potential is given y the following equation [Ca^{40}]:

$$J_0(E) = J_0(E_S)\exp\alpha(E-E_S) \quad (22)$$

Substituting Eq. (22) and Eq. (21) into Eq. (20), we get the value estimated in the first term of Eq. (3) according

to the following formula:

$$V_0(r,E) = \frac{J_0(E_S)}{g_V}[exp\ \propto_s (E - E_S)]\ f(r_V) \quad (23)$$

$f(r_V)$ has got the Woods-Saxon dependence shape, and is determined by the following relation:

$$f(r_V) = [1 + \exp(x_V)]^{-1} \quad ; x_V = \frac{r - R_V}{a_V};\ R_{V=}\ r_V A^{1/3}$$

Taking advantage of Eq. (15) and Eq. (23), the first term in Eq. (3) is rendered as follows:

$$V(r,E) = \frac{J_0(E_S)}{g_V}[exp\alpha(E - E_S)]f(r_V) + \Delta V_W(E)f(r_W) + \Delta V_d(E)g(r_d) \quad (24)$$

The second-order moment of real potential represents the sum of both the second-order moment of the potential $V_0(r,E)$ and the second-term moment of the dispersive potential as follows:

$$J_V(E) = J_0(E) + J_{\Delta V}(E) = J_0(E) + J_{\Delta V_w}(E) + J_{\Delta V_d}(E) \quad (25)$$

$J_{\Delta V_w}$- Second-order moment of the volume dispersive potential;

$J_{\Delta V_{wd}}$- Second-order moment of the surface dispersive potential

They are determined in accordance with the following Dispersion Relation:

$$J_{\Delta V}(E) = \frac{2}{\pi}(E - E_S)\int_{E_0}^{\infty} \frac{J_W(E`)dE`}{(E - E_S)^2 - (E` - E_S)^2} \quad (26)$$

As for the moment, $J_0(E)$, it is determined according to Eq. (22), which is rendered for convenience of all the preceding calculations by dividing the radius of Coulomb potential in accordance with the following Equation:

$$R_{C=}\ r_C A^{1/3} \quad (27)$$

Which is deemed $r_{C=}\ 1.25Fm$

The potential of the spin-orbit mutual effect is determined by the following equation:

$$V_{ls=} - V_{ls}\ (E)\ (4r_{ls}a_{ls})^{-1}\ g(x_{ls})\ \vec{L}\ .\ \vec{\sigma} \quad (28)$$

After finishing the determination of the mean nuclear field components, the reaction cross sections $\sigma_r(E)$, $\sigma(\theta)$ and $P(\theta)$ by using a program that is written by a Pascal language, in which case the real optical potential must be expressed by the parameters of Woods-Saxon optical potential as we are mentioned beforehand. Then, the linear extrapolation method of the Wood-Saxon potential must be made use of in accordance with the following equation:

$$V(r,E) = U_V\ (E)\ f(r_V)$$
$$U_{V=}\ V(r = 0, E) \quad (29)$$

In the framework of the VMA method, the real potential parameter (r_V) is deemed energy dependent, and its value is calculated by solving the following equation:

$$J_V(E) = \frac{4\pi R_V^3}{3A_P A_t}\left[1 + \frac{1}{3}\left(\frac{\pi a_V}{R_V(E)}\right)^2\right] U_V(E) \quad (30)$$

Where $J_V(E)$ is calculated according to Eq. (25), and $U_V(E)$ is calculated according to Eq. (24).

A special program related to the SPI-GENOA Program was prepared, and by which all the calculated values of $\sigma_r(E)$ are found, then the accurate determination thereof is ascertained by identifying them with their experimental counterparts at the same energy values.

Empirical Section:

In the framework of the VMA Method, the *at-issue* Al^{27} Nucleus is firstly characterized in pursuance of the experimental data that is available in the scientific references concerning the scattering of alpha (α) by the $\alpha + Al^{27}$ Interaction; viz. concerning the reaction total cross section $\sigma(E)$ and differential cross section $\sigma(\theta)$ and $P(\theta)$ within the deterministic range of energy at $(1 \le E_\alpha \le 10)MeV$.

The potential parameters were reached by the way of searching and simulating the calculated and experimental values of $\sigma(E)$ for the interaction $(\alpha + Al^{27})$ at the energy range $(1 \le E_\alpha \le 10)MeV$. They are listed in the following Table (1):

Table (1): The Results of the $\alpha + Al^{27}$ Interaction within the Range of Energy at $1 \le E_\alpha \le 10MeV$

E (MeV)	U_v (MeV)	r_v (Fm)	a_v (Fm)	W_w (MeV)	r_w (Fm)	a_w (Fm)
3	*80*	*2.099*	*0.766*	*10.5*	*1.43*	***0.65***
4	*79*	*1.871*	*0.618*	*13.5*	*1.435*	***0.655***
5	*78*	*1.76*	*0.592*	*16*	*1.44*	***0.66***
6	*77*	*1.759*	*0.571*	*17.7*	*1.445*	***0.67***
7	*76*	*1.758*	*0.564*	*19.2*	*1.45*	***0.675***
8	*75*	*1.757*	*0.558*	*19.8*	*1.455*	***0.68***
9	*74*	*1.756*	*0.55*	*20.7*	*1.46*	***0.685***
10	*73*	*1.755*	*0.544*	*21.7*	*1.465*	***0.69***

The values of the Optical Potential parameters, which were found for the System $(\alpha + Al^{27})$, were approved so that the cross section values, calculated by the SPI-GENOA Program, are highly approximate to the experimental values of the reaction cross section. In reliance on the foregoing, we set out the following tables that incorporate the values of the real second-order moments J_v and the imaginary second-order moments J_w that are fitted with the parameters previously calculated in Table (1) in addition to the cross section values of the Interaction $\alpha + Al^{27}$ at the range of energy under study.

Table (2): The Second-Order Moments by taking advantage of the OP Parameters of the $\alpha + Al^{27}$ Interaction

E (MeV)	σ (mb)	J_{ww} $(MeV.Fm^3)$	J_w $(MeV.Fm^3)$
3	3.20E+01	24.9	**24.9**
4	9.55E+01	23.37	**23.37**
5	2.53E+02	23.87	**23.87**
6	4.75E+02	23.37	**23.37**
7	6.71E+02	22.87	**22.87**
8	8.19E+02	22.37	**22.37**
9	9.29E+02	21.88	**21.88**
10	1.01E+03	21.4	**21.4**

DETERMINATION OF THE SECOND-ORDER MOMENT VALUES OF THE IMAGINARY PART OF THE SURFACE & VOLUME OPTICAL POTENTIAL:

In the framework of the VMA Method, the second-order moments are determined by using the Brown-Rho relation [6], namely:

1- The second-order total moment $J_W(E)$;

2- The volume imaginary potential $J_{W_W}(E)$;

For assurance of the accurate determination of the geometrical parameters of the optical potential and the accurate determination of the terms at the range of energy $(1 \le E_\alpha \le 10)MeV$, we compared the calculated values of the energy dependence of each of the second-order potential of the surface and volume imaginary part

with their experimental counterparts for the system $(\alpha + Al^{27})$. It is graphically represented as shown in Fig. (1):

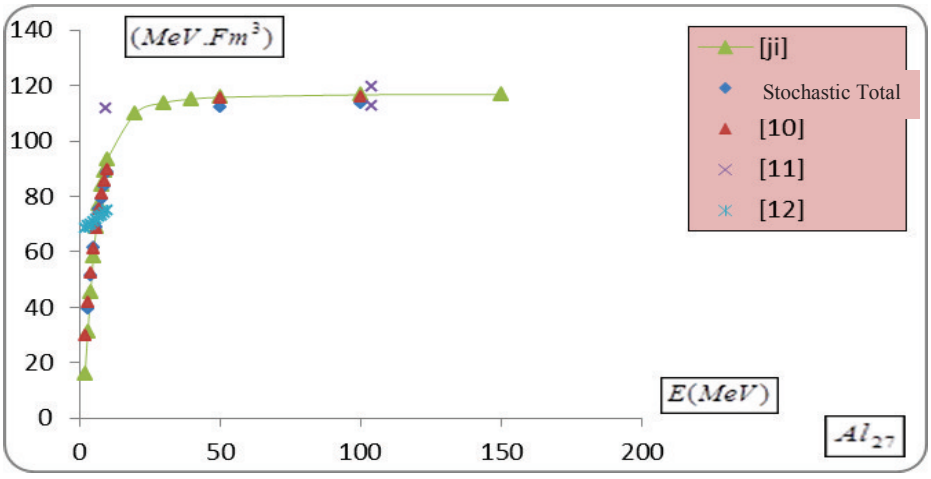

Figure (2) stands for the Second-Order Moment of the Imaginary-Part Optical Potential with its Energy Dependancy to the at-issue Nucleus, where (△), (X) & (*) are Moment Values in the References [10,11,12]

From Fig. (1), it is noted the calculated values of $J_W(E)$ are well identified with the data shown in the Reference[10], [12] and are clearly discordant with the Alpha-Perey Reference, since they are deemed among the classifications that have relied on expectancy (stochasticity) in selecting the optical potential parameters.

The Finding of the Real Potential in the Framework of the VMA Method:

After finding the parameters of $J_W(E)$ through drawing up the second-order moment of the imaginary potential in terms of energy, we conducted the fitting calculations in order to find the real moments for the $(Nucleus + \alpha)$ Interaction. They were compared afterwards with their experimental counterparts as shown in Fig. (2).

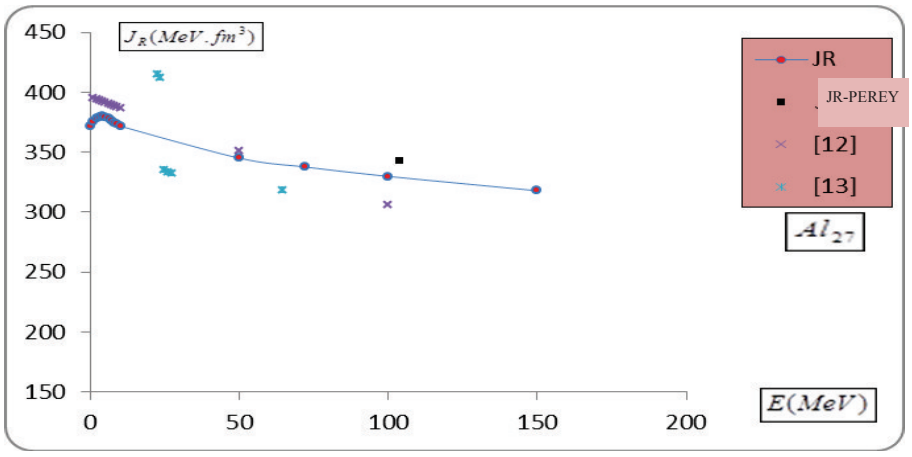

Figure (3) represents the Dependency of the Second-Order Moment of the real part of the Optical Potential for the Interaction $(\alpha + Al^{27})$ within the Range of Energy $(0 \leq E_\alpha \leq 200)MeV$

As noted from Fig. (2), there is a deviation in the energy dependence of the real moment at lower range of energies, and in particular in the energy threshold region of the interaction, and the interpretation of which is attributed to an anomaly, being resultant from the overlap of the real part with the imaginary part of the Dispersion Relation (DR).

The energy dependence of the dispersive moment for the interaction $(\alpha + Al^{27})$ was only determined through the Dispersion Relation (DR), which connects both the imaginary and real parts of OP within the range of energy

$(0 \leq E_\alpha \leq 200)\ MeV$ as shown in Fig. (3), which exhibits the Dispersion Relation of the Nucleus under study:

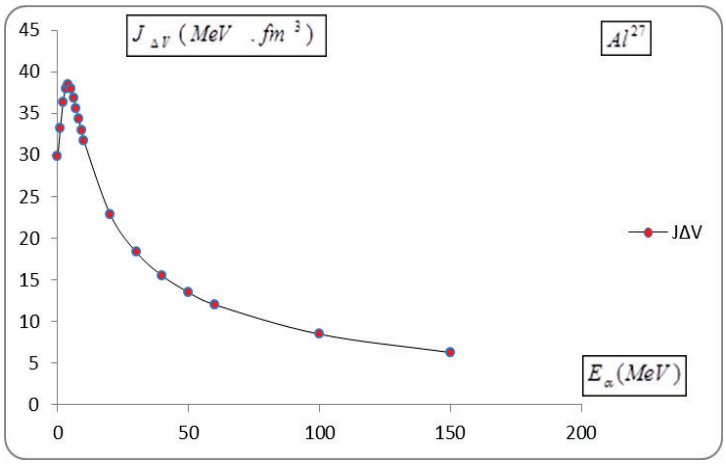

Figure (4) stands for the Energy-Dependence of the Dispersive Moment of tthe Interaction $(\square + Al^{27})$ at the Energy Range of $(0 \leq E_\alpha \leq 200)\ MeV$ as it is noted herein that it is in approximation of the Behavior of Real Moment near the Threshold, and which has a deviance in terms of Energy

DETERMINATION OF THE RADIAL VALUE OF THE REAL POTENTIAL (r_v) & STUDYING ITS ENERGY DEPENDENCE AT THE ENERGY RANGE OF $(1 \leq E_\alpha \leq 10)\ MeV$ IN THE FRAMEWORK OF THE VMA METHOD:

The Optical Real Potential radius for the Interaction is given by means of the following Third-Order Equation:

$$r_v^{\,3} = \frac{J_v(E)}{\left[1 + \frac{9.872}{A^{\frac{2}{3}}}\left(\frac{a_v}{r_v}\right)^2\right] \times V \times 4.156}$$

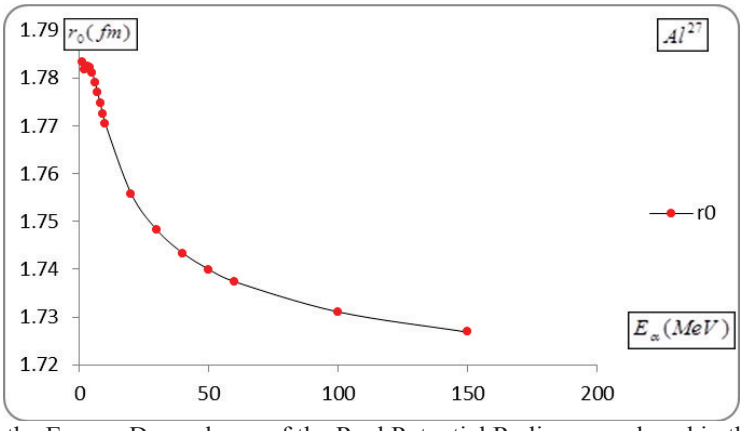

Figure (5) reveals the Energy Dependence of the Real Potential Radius reproduced in the Framework of the VMA Method

As it is noted, we find a remarkable rise in the low-range of energy near the Interaction Threshold, and a decline thereof with the increasing energy. This explains that at the threshold energy range there are reaction channels contributing in the mutual effects between the α-particle and the target nucleus. With the rise in energy, some channels are closed, and only a single channel is maintained: the scattering channel

Optical Potential Parameters in the Framework of the VMA Method:

After finding all the Parameters $U_V, r_V, a_V W_w, W_W, a_w$ and using the Property $a_w = a_d, r_w = r_d$, the reaction cross section value is calculated in accordance with these parameters, where such parameters are entered into the SPI-GENOA Program, and are then compared with their experimental counterparts in the following step.

Table (3): The Optical Potential Parameters of the Interaction $\alpha + Al_{13}^{27}$ resultant in the Framework of the VMA Method

E (MeV)	U_v (MeV)	r_v (fm)	a_v (fm)	W_w) MeV (	r_w (fm)	a_w (fm)	σ (mb)	J_R $(MeV.Fm^3)$	J_w $(MeV.Fm^3)$
3	60.43	1.7823	0.56	7.49	1.45	0.68	2.01	396.77	39.41
4	60.48	1.78218	0.56	11.255	1.45	0.68	42.4	396.97	51.28
5	60.49	1.7809	0.56	14.577	1.45	0.68	209	396.29	61.51
6	60.47	1.7791	0.56	17.318	1.45	0.68	441	395.04	68.86
7	60.45	1.7769	0.56	19.51	1.45	0.68	645	393.42	75.59
8	60.43	1.7747	0.56	21.245	1.45	0.68	802	392.05	79.11
9	60.4	1.772	0.56	22.617	1.45	0.68	922	390.18	83.69
10	60.37	1.77	0.56	23.708	1.45	0.68	1016	388	88.77

Determination (Calculation) of the Cross Section of the Reaction $\alpha + Al_{13}^{27}$ by using the Optical Potential Parameters reproduced in the Framework of the VMA Method:

After finding the Optical Potential (and its Parameters) resultant from the mutual effects between the α-projectiles towards the target (Al^{27}), we conducted the following:

First: Calculation of the Cross section of the Reaction $(\alpha + Al^{27})$ within the range of energy at $(1 \leq E_\alpha \leq 10)\ MeV$. It is followed by their comparison with their experimental counterparts at the same range of energy under study as shown in Fig. (5):

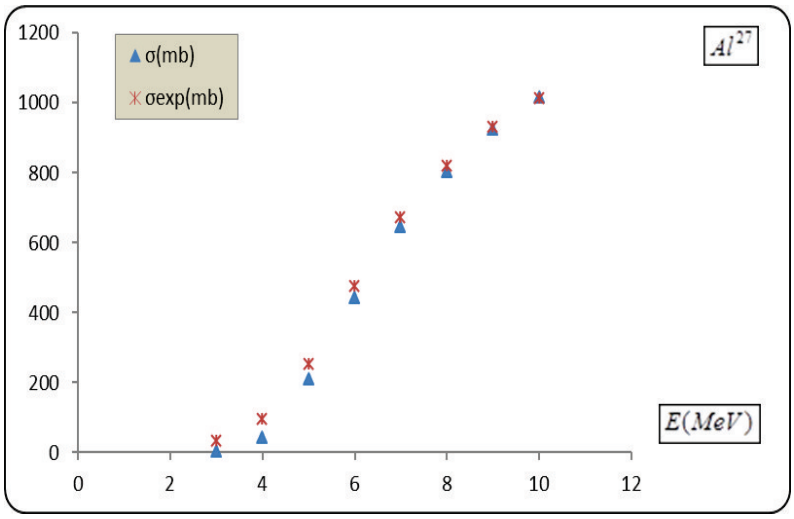

Figure (6) stands for the Energy Dependences of the Cross Section and of the Interaction $(\alpha + Al^{27})$ at the Energy Range $(1 \leq E_\alpha \leq 10)\ MeV$, which is calculated by using the As-Amended VMA, and the comparison thereof with their Experimental Counterparts in Reference [14]

As shown in Fig. (5), it is noted that the calculated and experimental values of the cross section of the Reaction $(\alpha + Al^{27})$ are fitted at the range of energy under study and within the permitted experimental errors.

Second: Calculation of the Differential Cross section of the Reaction $(\alpha + Al^{27})$ for the Energy $E_\alpha = 10MeV$ and studying its Angular Dependence as() shown in Fig. (6).

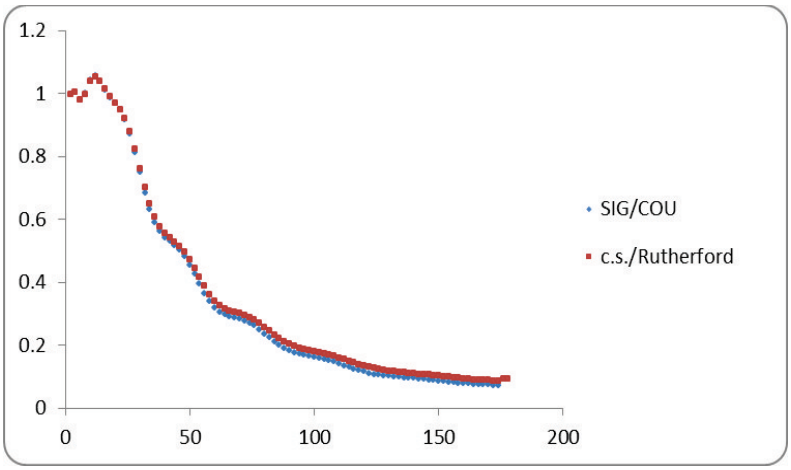

Figure (7) stands for the Angular Dependence of the Differential Cross Section of the Reactin $(\alpha + \mathrm{Al}^{27})$ for the Energy $\mathrm{E}_{\alpha} = 10\mathrm{MeV}$, which is calculated by using the As-Amended VMA Method and the comparison thereof with its Experimental Counterparts [15]

In Fig. (6), it is noted that the calculated and experimental values of the differential cross section of the Reaction $(\alpha + Al^{27})$ are fitted for the small and large angles and they have been behaving on the same lines. Therefore, we can say that the differential cross section is so sensitive for the nuclear potential shape that is fitted at the higher range of energy than the Coulomb barrier.

From Fig. (5) and Fig. (6), we can say that the fit is so convincing since the dispersive mean field incorporates only so little adjustable parameters. In addition, if the parametric identifications are effected at each energy independently, they will be not as good as being resultant in the actually-effected extent, and this refers to the following truism:

The quality of nuclear structure effects plays a more significant role in the lightweight nuclei than heavyweight nuclei. In addition, the Woods-Saxon radial shape may be so simple in case of the lightweight nuclei.

The preceding figures (3,4,5,6) corroborates the reliability of the dispersive mean field. Furthermore, the approximate resemblance between the experimental results and those reproduced from the Dispersive Optical Model Analysis proves the accuracy of the method having been made use of.

Conclusions

1. For the first time, the As-amended VMA Method is used to analyze the differential cross section with its angular dependence $\sigma(\theta)$ and polarization $P(\theta)$, and the reaction total cross section with its energy dependence at the energy range of $(1 \leq E_{\alpha} \leq 10)$ for the System $(\alpha + Al^{27})$.
2. We found out that the values of the second-order moment of the real part are fitted and identified with their counterparts in References [ ] for the Interaction $(\alpha + Al^{27})$ within the range of energy at $(1 \leq E_{\alpha} \leq 10)\ MeV$.
3. We found out that the values of the second-order moment of the imaginary part are fitted and identified with their counterparts in References [10,11,12] for the Interaction $(\alpha + Al^{27})$ within the range of energy at $(1 \leq E_{\alpha} \leq 10)\ MeV$ for instance.
4. We further found out a heterogeneous behavior in the second-order moment of the real part for the System $(\alpha + Al^{27})$ within the range of energy near the Coulomb barrier (the Energy Threshold). Such behavior consists in an anomaly for the energy dependence of the Potential $J_R(E)$.
5. We further found out a heterogeneous behavior in the energy dependence of the Optical Potential radius near the Energy Threshold. This can be explained as result of the Dispersion Relation (DR) that connects both real and imaginary parts of Potential, where such anomaly is exhibited due to the closure of some reaction channels.
6. After calculating the reaction total cross section, we found it out to be identified with its experimental counterparts for the System $(\alpha + Al^{27})$ and within the energy range at $(1 \leq E_{\alpha} \leq 10)\ MeV$.
7. After calculating the Differential Cross section of the Reaction as angularly dependent, we found it out to

be fitted and have a homogeneous behavior upon comparing it with its counterparts that are extracted from References [15], wherewith the accurate determination of the Optical Potential Parameters as well as the accuracy and authenticity of the utilized Method are assured.

Recommendations

1) To use the As-amended VMA Method in studying a widespread spectrum of nuclei at different ranges of energy for the $^{4}_{2}He$ projectiles;
2) To extend the Study to incorporate heaviest heavy-ions of $^{4}_{2}He$.

References

[1] Mahaux, c.,& Sartor ,R.(1991). Dispersion Relation Approach to the Mean Field and Spectral Functions of Nucleus in Ca^{40}. Nucl. Phys. V. A52,P. 253-297.

[2] Hodgson, P., E, (1992)The Dispersive Optical Model, Ounp, P. P. 1-7.

[3] Романовский, E.,& A. , Becpalova B.(2004) Analyzed Within the Dispersive Optical Model for the Proton And Zr^{90} Within Energies 5MeV <E<65MeV, Nucl. Phys. 2004

[4] M. Nolte., &H. Machner, (1987) Global Optical Potential For a Particles with Energies Above 80 MeV, Physical Review c Volume 36,Number 4 October.

[5] Baeza, A.,& Bilwes, B. (1984)Energy-Dependent enormalization Coefficients of Folding-Model Description of 32S+ 40Ca elastic Scattering,Nuclear Physics, Section A, Volume 419, Issue 2, p. 412-428.

[6] Mahaux, C.,& Satchler, G.,R.(1986) Radial And Energy Dependence Of The Dispersive Contributions To The (α +160 And Lα +40Ca Potentials Near The Threshold Anomaly, Nuclear Physics A456, 134-158.

[7] Mahaux . C.,Sartor . R ,(1992) -Advance in Nuclear, phys. edited , New. York , Vol . 20 , p.1.

[8] A. J. Koning., J. P. Delarocheb.(2003) Local and global nucleon optical models from 1Kev to 200 Mev. Nuclear physics. A713231-310.

[9] Brown. E. G., and Rho. M., Nucl Phys. A 458, 25. 1986.

[10] A. Shridhar., N, Lingappa, (1980) Systematics in the Volume Integrals of The Imaginary Part of the Alpha-Nucleus Optical Potentials, Physical Review C.

[11] C. M. Perey., & F. G. Perey. (1976). Compilation Of PhenomenologIcal Optical-Model Parameters* Atomic Data And Nuclear Data Tables.

[12] M. E. Cage., A. J. Cole (1972) Ambigities And Systematics In The Real Central Part Of The Optical-Model Potential.Nuclear Physies

[13] M.N.A. Abdullah., M.S. Mahbub. (2002)Investigation of α-nucleus interaction in the 27Al(α, α)27Al scattering and 27Al(α, d)29Si The European Physical Journal A.

[14] Acselam Library **(C)**Copyright, (1998)Jaer**.** Table of Isotope Production Cross Sections.

[15] A.J. Koning,.& D. Rochman. (2015). TALYS-based evaluated nuclear data library.